Toxicology 511 (2025) 154066

Contents lists available at ScienceDirect

Toxicology

journal homepage: www.elsevier.com/locate/toxicol

Assessing the impact of TiO_2 nanomaterials on intestinal cells: New evidence for epithelial translocation and potential pro-inflammatory effects

Dora Rolo [a,b], Joana F.S. Pereira [a,d], Lídia Gonçalves [c], Ana Bettencourt [c], Peter Jordan [a,d], Maria João Silva [a,b,1], Paulo Matos [a,d,1], Henriqueta Louro [a,b,*,1]

[a] National Institute of Health Doutor Ricardo Jorge, I.P (INSA), Department of Human Genetics, Lisbon, Portugal
[b] bCentre for Toxicogenomics and Human Health (ToxOmics), NOVA Medical School, Universidade NOVA de Lisboa, Lisbon, Portugal
[c] Research Institute for Medicines (iMed.ULisboa), Faculty of Pharmacy, Universidade de Lisboa, Lisboa 1649-003, Portugal
[d] BioISI – Biosystems & Integrative Sciences Institute, Faculty of Sciences, University of Lisboa, Lisboa 1749-016, Portugal

ARTICLE INFO

Handling Editor: Dr. Mathieu Vinken

Keywords:
Titanium dioxide
Ingested Nanomaterials
Epithelial barrier
GIT
Digestion
Transcytosis

ABSTRACT

Understanding the potential impact of nanomaterials (NMs) on human health requires further investigation into the organ-specific nano-bio interplay at the cellular and molecular levels. We showed increased chromosomal damage in intestinal cells exposed to some of *in vitro* digested Titanium dioxide (TiO_2) NMs. The present study aimed to explore possible mechanisms linked to the uptake, epithelial barrier integrity, cellular trafficking, as well as activation of pro-inflammatory pathways, after exposure to three TiO_2-NMs (NM-102, NM-103, and NM-105).

Using confocal microscopy, we show that all NMs, digested or not, were able to enter different types of intestinal cells. At the physiologically relevant concentration of 14 µg/mL, the digested TiO_2-NMs did not compromise the transepithelial resistance, nor the levels of epithelial markers E-cadherin and Zonula occludens protein 1 (ZO-1), of polarized enterocyte monolayers. Nonetheless, all NMs were internalized by intestinal cells and, while NM-102 was retained in lysosomes, NM-103 and NM-105 were able to transverse the epithelial barrier through transcytosis. Moreover, 24 h exposure of 14 and 1.4 µg/mL digested NM-105, promoted interleukin IL-1β expression in activated M1 macrophages, indicating a potential pro-inflammatory action in the gut.

Taken together, our findings shed light on the cell-specific nano-bio interplay of TiO_2-NMs in the context of the intestinal tract and highlight transcytosis as a potential gateway for their systemic distribution. The potential pro-inflammatory action of digested NM-105 emphasizes the importance of pursuing research into the potential impact of NMs on human health and contribute to the weight of evidence to limit their use in food.

1. Introduction

Nanomaterials, including titanium dioxide (TiO_2-NMs), are commonly present in many consumer products. They can be ingested either directly through products or pharmaceuticals containing NMs, or indirectly through food contaminated with NMs released from food-contact materials or environmental accumulation (Huang et al. 2018). As a result, the gastrointestinal tract (GIT) is a likely site of contact of NMs, which may lead to systemic exposure if the GIT barriers is breached (Rice, 2022) or if the NMs are able to cross the barrier through other mechanisms. Despite this knowledge, the potential toxicity of TiO_2-NMs in the GIT has not been fully elucidated, with some studies showing evidence of genotoxicity in intestinal cells, and other studies yielding contradictory results (EFSA, 2021).

An integrative analysis of the published data on cellular and molecular mechanisms triggered after the ingestion of TiO_2-NMs was published by our research group (Rolo et al. 2022). We have proposed adverse outcome pathways (AOPs) linking key events such as oxidative stress, DNA/ chromosomal damage, cell death, and inflammation, leading to a possible systemic distribution. Two AOPs were proposed, where colorectal cancer, liver injury, reproductive toxicity, cardiac and kidney damage, as well as hematological effects, stand out as possible

* Correspondence to: National Institute of Health Doutor Ricardo Jorge, I.P (INSA), Department of Human Genetics, Avenida Padre Cruz, Lisbon 1649-016, Portugal.
E-mail address: henriqueta.louro@insa.min-saude.pt (H. Louro).
[1] Co-senior authors

https://doi.org/10.1016/j.tox.2025.154066
Received 6 September 2024; Received in revised form 14 January 2025; Accepted 23 January 2025
Available online 25 January 2025

adverse outcomes. While several *in vivo* studies have indicated that TiO_2-NMs can cross the GIT barrier and cause systemic effects, the crossing mechanism is still controversial. In addition, the *in vitro* cellular studies characterizing those mechanisms used TiO_2-NMs that had not been subjected to the digestive process (Rolo et al. 2022). To include the digestion process in the comparative toxicity assessment of TiO_2-NMs, we have previously described the application of the standardized static INFOGEST 2.0 *in vitro* digestion method (Brodkorb et al. 2019) to three different TiO_2-NMs (NM-102, NM-103 and NM-105), at physiologically relevant concentrations for the human intestine (Bettencourt et al., 2020). Remarkably, the hydrodynamic size of NM-105 decreased after digestion and, compared with the pristine form, a more toxic effect occurred in HT29-MTX-E12 mucous-secreting colorectal cancer cells (Bettencourt et al., 2020). Furthermore, recent results evidenced a DNA-damaging effect dependent on the NM, more relevant for the rutile/anatase NM-105, possibly due to its lower hydrodynamic size in the cells' medium (Vieira et al. 2022). The mechanisms behind these observations, however, remained unclear.

The present study aimed to explore possible mechanisms linked to NMs' uptake, epithelial barrier integrity, cellular trafficking, as well as activation of pro-inflammatory pathways. We characterized the mechanisms mediating the crossing of the epithelial barrier by TiO_2-NMs and recognized digested NM-105 as a potential novel mediator of pro-inflammatory pathways in the GIT.

2. Materials and methods

2.1. TiO_2-NMs sample preparation

The three TiO_2-NMs used in this work, NM-102, NM-103 and NM-105, were kindly provided by the Joint Research Centre (JRC, Ispra, Italy) and are considered as international benchmarks (JRC 2014), and prepared under good laboratory practices (GLP). Their primary physicochemical characteristics were provided by JRC (JRC 2014) and are described in and are summarized in Bettencourt et al. (2020). Briefly, these three TiO_2 have distinct crystalline structures (anatase or rutile or mixture of anatase and rutile) and different sizes, specific surface area and agglomerates' size. In addition, NM-103 is hydrophobic, Al-coated, while others are uncoated. NM-105 (also known as Aeroxide P25) exhibits mixed crystallinity, with anatase as the predominant form (81.5 % anatase: 18.5 % rutile). The characteristics in cell culture media can be found in Bettencourt et al. (2020).

For each biological assay, a 2.56 mg/mL stock dispersion of each NM was prepared as previously described (Vieira et al. 2022), by prewetting powder in 0.5 % absolute ethanol (96 %) followed by addition of sterile-filtered 0.05 wt% bovine serum albumin (BSA)-water and dispersion by 16 min of probe sonication of the sample with a 400- Watt Branson Sonifier S-450D (Branson Ultrasonics Corp., Danbury, CT, USA), cooled in an ice-water bath. The stock dispersions were immediately used either for the static digestion process (Brodkorb et al. 2019), being digested samples (named DIG) or directly (undigested samples) for biological assays, after dilution in cell culture medium Dulbecco's modified Eagle medium (DMEM), and following the most recent recommendations (Vital et al. 2024).

2.2. Intestinal cell lines assays

2.2.1. Cell Culture

Caco-2 and HT29-MTX-E12 cells were maintained in DMEM cell medium. The media were supplemented 1 % penicillin/streptomycin (10,000 U/mL), 2.5 % HEPES buffer, 10 % fetal bovine serum (FBS) and 1 % fungizone (all reagents were from Thermo Fisher Scientific, Waltham, MA, USA). Cells were maintained at 37°C with 5 % CO_2, and regularly checked for an absence of mycoplasma infection by PCR amplification of a 16S ribosomal DNA fragment (primers forward (F) 5′ ACTCCTACGGGAGGCAGCAGTA 3′ and reverse (R) 5′ TGCACCATCTGTCACTCTGTTAACCTC 3′) from lysates of cells harvested from the culture medium.

2.2.2. Cell polarization

For cell polarization, Caco-2 cells were grown on porous (1 μm) transwell polyester (PET) filter inserts (24-well size, 6.4 mm diameter and 0.3 cm^2 area, Corning) in DMEM medium supplemented with 5 % (v/v) FBS for 21 days, until they reached a transepithelial electrical resistance (TEER) of ~600 Ω. cm^2, as measured with a chopstick electrode STX2 (World Precision Instruments, Sarasota, FL, USA) (Pereira et al. 2022).

2.2.3. Fluorescence assays

TiO_2-NMs were conjugated with the fluorescent Alizarin Red S (ARS) dye (as described at (Thurn et al. 2009)). Briefly, to 1 mL of the stock solution of the NMs was added 200 μL of the ARS stain kit solution (GeneCopeia, MD, USA) and incubated 4 h at room temperature with shaking. After this period, the free dye was removed by washing three times the NMs with 1 mL of sterile purified water followed by centrifugation (10 min at 12,000 g at room temperature). Finally, they were resuspended in 1 mL of sterile purified water and preserved at 4°C.

When the cell monolayers were prepared, the media from both compartments of the Transwell inserts were removed. The basolateral chambers were filled with 0.5 mL of fresh DMEM medium supplemented with 5 %FBS, and the apical compartment was covered with 0.5 mL of NMs (digested or not) at 14 μg/mL and 100 μg/m, diluted in DMEM medium with 5 %FBS, during 24 h. When 0.5 mL of NMs suspension was added to the 0.33 cm^2 Transwell inserts, the cells were therefore exposed to $3x10^{10}$ particles/cm^2 (at 14 μg/mL). The fluorescence of the NMs were analyzed before and after 24 h exposure, recovering independently the media collected from both compartments of the inserts (apical and basolateral). The 3 independent measurements were performed with a microplate multi-mode reader (FLUOstarOmega, BMGLabtech, Germany) at a fluorescence excitation wavelength at 520 nm and an emission wavelength at 586 nm.

2.2.4. Confocal immunofluorescence microscopy

Caco-2 and HT29-MTX-E12 cell lines grown either on coverslips or on PET filters, were treated as indicated, washed twice in PBS, immediately fixed with 4 % (v/v) formaldehyde in PBS for 20 min at room temperature, and subsequently permeabilized with 0.5 % (v/v) Triton X-100 in PBS for 30 min at room temperature. When indicated, cells were then labeled for 2 h with primary antibodies against early-endosome antigen 1 (EEA1, E-8 clone), lysosome-associated membrane protein-1 (LAMP1, H4A3 clone), Ras-related in brain protein 7 (RAB7, B-3 clone), all from Santa Cruz Biotechnology (Santa Cruz, CA, USA), or lysobisphosphatidic acid (LBPA, 6C4 clone, Millipore, Burlington, MA, EUA) and washed 3 × in PBST (PBS + 0.01 % Tx-100) for 5 min with gentle shaking, followed by 30 min incubation with a 1:500 dilution of mouse or rabbit Alexa Fluor 488 (Thermo Fisher Scientific, Waltham, MA, USA) and phalloidin-FITC (Sigma-Aldrich, St. Louis, MO, USA). Cells were washed 3 × in PBS, briefly stained with 1.25 μg/mL DAPI (Sigma-Aldrich, St. Louis, MO, USA), washed again, post-fixed with 4 % (v/v) formaldehyde in PBS for 10 min at room temperature. Then coverslips, or PET filters covered by coverslips, were mounted on glass slides in VectaShield (Vector Laboratories, Burlingame, CA, USA) and sealed with nail polish. The 405 nm, 488 nm and 532 nm laser lines of a Leica TCS-SPE confocal microscope were used to acquire one Airy thick Z-axis stacks of XY-plane images (from the bottom to the top of the cultured cells), to enable reconstruction and visualization of the entire cytoplasm in the XZ plane. Recorded images were processed with Leica in-built software and assembled in figures with Adobe Photoshop software (CS4, version 11.0), and the raw (Leica Lif format) data files with all image stacks from where the representative generated images are shared as Supplementary Material.

2.2.5. Western blot (WB) procedures

Cells were in PET filters were lysed in 50 μL of Laemmli sample buffer (containing 50 μL of lysis buffer [50 mM Tris/HCl (pH 7.5), 2 mM MgCl2, 100 mM NaCl, 10 % (v/v) glycerol, 1 % (v/v) NP40]) and total protein extracts were separated in 10 % (w/v) SDS-PAGE gels. Following electrophoresis, proteins were transferred onto a polyvinylidene difluoride (PVDF) membrane (Bio-Rad, Hercules, CA, USA). Membranes were blocked in 5 % (w/v) milk powder in wash buffer (TBS with 0.5 % (v/v) Triton X-100) and specific proteins probed overnight using primary antibodies against: α-tubulin (Clone B-5–1–2; both from Sigma-Aldrich, St. Louis, MO, USA), E-cadherin (BD Biosciences, San Carlos, CA, USA), Zonula occludens protein 1 (ZO-1) (clone H-300; Santa Cruz Biotechnology, Santa Cruz, CA, USA). Following, three wash steps, membranes were incubated with a goat anti-mouse or anti-rabbit IgG horseradish peroxidase conjugate (Bio-Rad, Hercules, CA, USA). Protein bands were visualized by chemiluminescence on X-ray films and quantified on digitized images by densitometric analysis with ImageJ software (version 1.53f51, National Institutes of Health, Bethesda, MD, USA). All original WB film exposures used to assemble the Figures can be found in the Supplementary Materials (Uncropped_WBs_V2.pdf).

2.3. Macrophage activation assays

2.3.1. THP-1 cell culture and differentiation

THP-1 monocyte cells were maintained in Roswell Park Memorial Institute 1640 Medium (RPMI) (high glucose, with Glutamax, no HEPES nor Sodium Pyruvate – 61870), supplemented with 10 % (v/v) of Heat inactivated FBS (16,140) and maintained at 37°C with 5 % CO_2 in 6-well plates. Cells were regularly checked for an absence of mycoplasma infection, as above. THP-1 monocytes were differentiated as previously described (Pereira et al. 2022). Briefly, differentiation to resting M0 macrophages was achieved with 50 ng/mL phorbol-12-myristate 13-acetate (PMA) (Sigma-Aldrich, St. Louis, MO, USA) for 24 h. Afterwards, M0 cells were placed for 24 h with fresh medium supplemented with 10 ng/mL Lipopolysaccharide (LPS, L4516 Sigma-Aldrich, St. Louis, MO, USA) and 10 ng/mL interferon gamma (IFN)-γ (Gibco, Thermo Fisher Scientific, Waltham, MA, USA), to induce pro-inflammatory M1 macrophages differentiation. After an additional 24 h of differentiation, the cells were exposed to NMs, with treatment-free medium.

2.3.2. Quantification of IL-1β expression

After 24 h of exposure with the indicated TiO_2-NMs (at 14 μg/mL and 1.4 μg/mL), total RNA was extracted from M0 and M1 cells with a RNA isolation kit (Macharey-Nagel, Düren, Germany) and reverse transcribed using random primers (Thermo Fisher Scientific, Waltham, MA, USA) and Ready-to-Go You-Prime First Strand Beads (Cytiva, Marlborough, MA, USA). Quantification of the proinflammatory cytokine interleukin 1-β (IL-1β) mRNA levels was performed using qRT-PCR and the $2^{-\Delta\Delta Ct}$ method, with GAPDH transcript as internal control, as previously described (Pereira et al. 2022). For statistical analysis, relative IL-1β expression values were compared between mock (BSA) treatments and 1.4 and 14 μg/mL concentrations of each NM, both digested and undigested, in M0 and M1 macrophage cells. Statistical comparisons were performed using two-way ANOVA followed by Bonferroni post-hoc tests, as described in the following section.

2.4. Statistical analysis

We analyzed the data using Student's T-test for paired group comparisons. For multiple group comparisons, we employed either one-way or two-way ANOVA, followed by Tukey's or Bonferroni post-hoc tests, respectively. Statistical significance was set at $p < 0.05$. Results are presented as mean ± SD, derived from three independent experiments.

3. Results and discussion

3.1. Uptake of TiO_2-NMs by intestinal cells

In order to test if TiO_2-NMs are internalized by the intestinal cells, we used confocal microscopy to observe the cellular localization of the three TiO_2-NMs fluorescent Alizarin conjugated, after 24 h of exposure to 14 μg/mL, digested or undigested, in Caco-2 and HT29-MTX-E12 intestinal cell lines (Fig. 1). The confocal images shown are representative of the observations collected in two independent experiments for each condition, for each cell line. In each case, stacks of 30–48 images were acquired, depending on sample thickness, and analyzed within the Leica software. The most representative XZ images were selected through the snapshot function and used to illustrate the observed trends.

This analysis showed that signals from all three NMs, either digested or undigested, could be seen inside the cytoplasm of HT29-MTX-E12 cells (Fig. 1A), but only sporadic signals of internalized NMs could be detected in Caco-2 cells (Fig. 1B). In a previous study, we have shown that exposure to TiO_2-NMs induced a significant increase in chromosomal damage, an indicator of cancer risk, in HT29-MTX-E12 cells, particularly when the NMs were first subjected to *in vitro* digestion procedure (Vieira et al. 2022). The present confocal microscopy observations suggest that such effects can be associated with the presence of the NMs in the cytoplasm of the mucous-secreting colonic cells that apparently does not require the translocation from the cytoplasm to nucleus. Although during mitosis the genetic material is exposed since the cell loses nuclear membrane, our findings are suggestive also of an indirect mechanism leading to the observed genotoxic effects. Conversely, in a publication considering food-grade TiO_2-NMs (Talbot et al., 2018), NMs are trapped by intestinal mucus by mucus-secreting HT29-MTX-E12 intestinal epithelial cells, suggesting that mucus presence reduces uptake.

In the literature, ROS have been pointed as plausible mechanism for

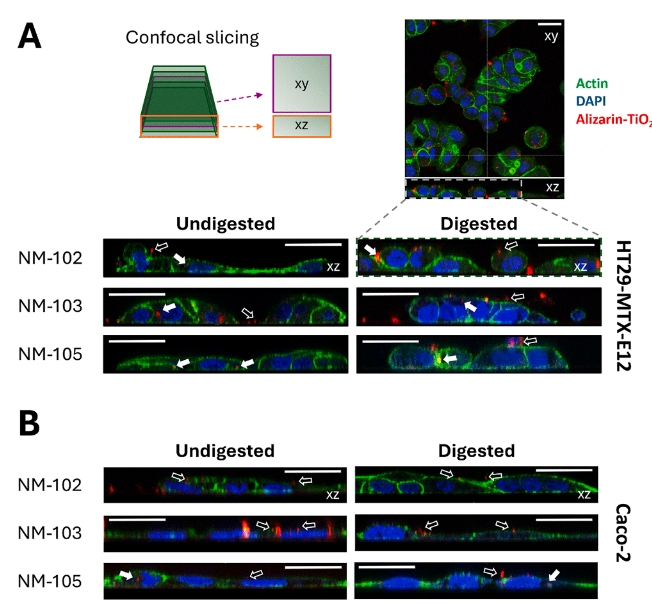

Fig. 1. Assessment of TiO_2-NM uptake by (A) HT29-MTX-E12 and (B) Caco-2 colonic cells. Cells were exposed for 24 h to 14 μg/mL of Alizarin-conjugated TiO_2 nanoparticles NM-102, NM-103, or NM-105 (red signals). The NMs were either applied directly (undigested) or after being subjected to INFOGEST 2.0 in vitro digestion (digested). Cells were stained with FITC-phalloidin for actin (green signals) and DAPI for nuclei (blue signals). Shown are XZ plane images generated from Z-stacks of XY-plane confocal images, allowing visualization of the entire cytoplasm (see diagram and representative XY image in (A)). Filled arrows indicate NM signals inside cells; hollow arrows indicate NM signals outside cells. White horizontal bars represent 25 μm.

their genotoxicity since in some reports TiO_2-NMs have a tendency to generate free hydroxyl radicals leading to oxidative stress-mediated genotoxicity and, ultimately, to apoptosis (Shukla et al. 2014; Azim et al. 2015). However, our previous studies (Vieira et al. 2022) showed the absence of ROS induction in HT29-MTX-E12 cells exposed to physiologically relevant concentrations of the same TiO_2-NMs samples. Likewise, Cao et al. (2019) did not find any signs of oxidative stress and ROS production, and other mechanisms were assumed to have led to the toxic responses reported.

The present findings of the low internalization of TiO_2-NMs in Caco-2 cells, is also consistent with mostly negative findings on chromosomal and DNA damage (Vieira et al. 2022). Briefly, the results suggest that digested NM-105, induces an increase in DNA damage in Caco-2 and HT-29-MTX-E12 cell lines, but NM-102, NM-103 and NM-105 exposure leads to chromosomal damage only in HT29-MTX-E12, an effect that is maintained by the digested NMs. These observations led us to hypothesize that the inability of the absorptive Caco-2 cells to internalizeTiO_2-NMs be due to a lack of enterocyte-like differentiation and polarization, and this issue needed further investigation.

3.2. *Uptake of TiO2-NMs in polarized enterocytes and effects in epithelial barrier integrity*

Caco-2 cells can be polarized *in vitro* into tight epithelial monolayers that are widely accepted as models to study intestinal permeability and the associated physiological processes (Costa and Ahluwalia, 2019). The tight junctions between polarized enterocytes, the absorptive epithelial cells that line the gut (Koch and Nusrat, 2009), maintain the integrity of the intestinal barrier.

We prepared polarized Caco-2 cells for 18 days until they reached a

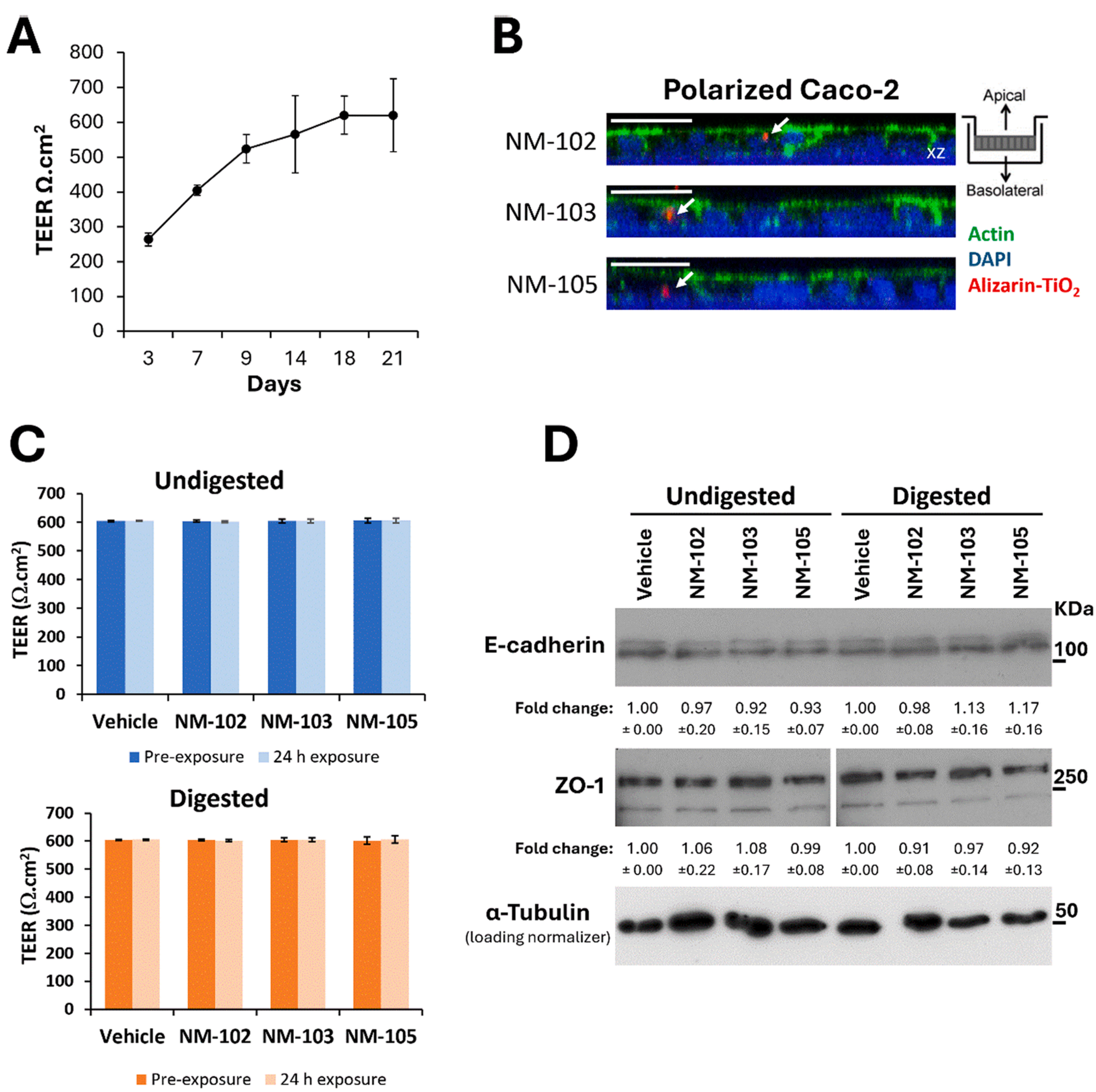

Fig. 2. Effect of 14 μg/mL TiO2-NMs on epithelial barrier properties of polarized Caco-2 monolayers. (A) Transepithelial electrical resistance (TEER) measured across Caco-2 monolayers for 21 days post-seeding on PET transwell filters. (B) Confocal images showing XZ cross-sections of polarized Caco-2 monolayers after 24 h of exposure to 14 μg/mL of Alizarin-conjugated TiO_2 nanoparticles NM-102, NM-103, or NM-105. Cells were stained with FITC-phalloidin (green) and DAPI (blue). Red signals indicate the presence of Alizarin-conjugated NMs. Arrows indicate internalized TiO_2-NM aggregates. White horizontal bars represent 25 μm. (C) Comparison of TEER values in fully polarized Caco-2 monolayers before and after 24-h exposure to 14 μg/mL of INFOGEST 2.0-digested or undigested TiO_2-NMs, as indicated. Values represent means ± SD from at least three independent experiments. (D) Western blot analysis of epithelial markers E-cadherin and Zonula occludens-1 (ZO-1) in cell lysates from polarized Caco-2 monolayers treated as described in (C). Quantification of WB band densities (mean ± SD) from three independent experiments is shown below each panel, normalized to α-tubulin levels (loading control).

transepithelial electrical resistance (TEER) of ~600 Ω.cm^2, which was sustained with onward culturing up to 21 days (Fig. 2A). After reaching a stable TEER, the monolayers were exposed to the tested TiO_2-NMs. Staining of polarized cells with FITC-labelled phalloidin showed a columnar-like morphology with clear basolateral and apical membrane domains (Fig. 2B), as previously described (Iftikhar et al. 2020). Moreover, consistent with our hypothesis, 24 h of exposure of fully polarized Caco-2 monolayers to 14 μg/mL of either NM-102, NM-103, or NM-105, ingested or not, revealed the presence of aggregates of these NMs, exceeding 1 μm in diameter, within the cells' cytoplasm, clearly indicating active internalization (Fig. 2B).

We did not find any significant variation in TEER values comparing pre- and post-exposure conditions with neither of the NMs, either undigested or digested (Fig. 2C). This observation suggests that the exposure of fully polarized Caco-2 monolayers to NM-102, NM-103, or NM-105 (digested, or not) does not affect their integrity or epithelial barrier properties. The same absence of alterations were observed at the two tested NMs concentrations (14 and 100 μg/mL). However, other studies have suggested that TiO_2-NMs ingestion can alter the intestinal barrier, and that these NMs can enter and be distributed through the blood stream and accumulate in several organs (EFSA, 2021). In a study from 2010 (Koeneman et al. 2010), the acute exposure of Caco-2 did not have any significant effect on the TEER, while after the chronic exposure of TiO2-NMs (reapplication for 10 days) the TEER dropped significantly, although the cells did begin to recover, after time, from this treatment. Some authors (Malaisé et al. 2024) have shown that the integrity of the gut barrier, in terms of cell proliferation/differentiation, genotoxicity, and epithelial tight junctions, is altered in murine and pig models after exposure to different small TiO_2-NMs with anatase crystal form, similar to NM-102 (Vignard et al. 2023). It was also reported that food-grade

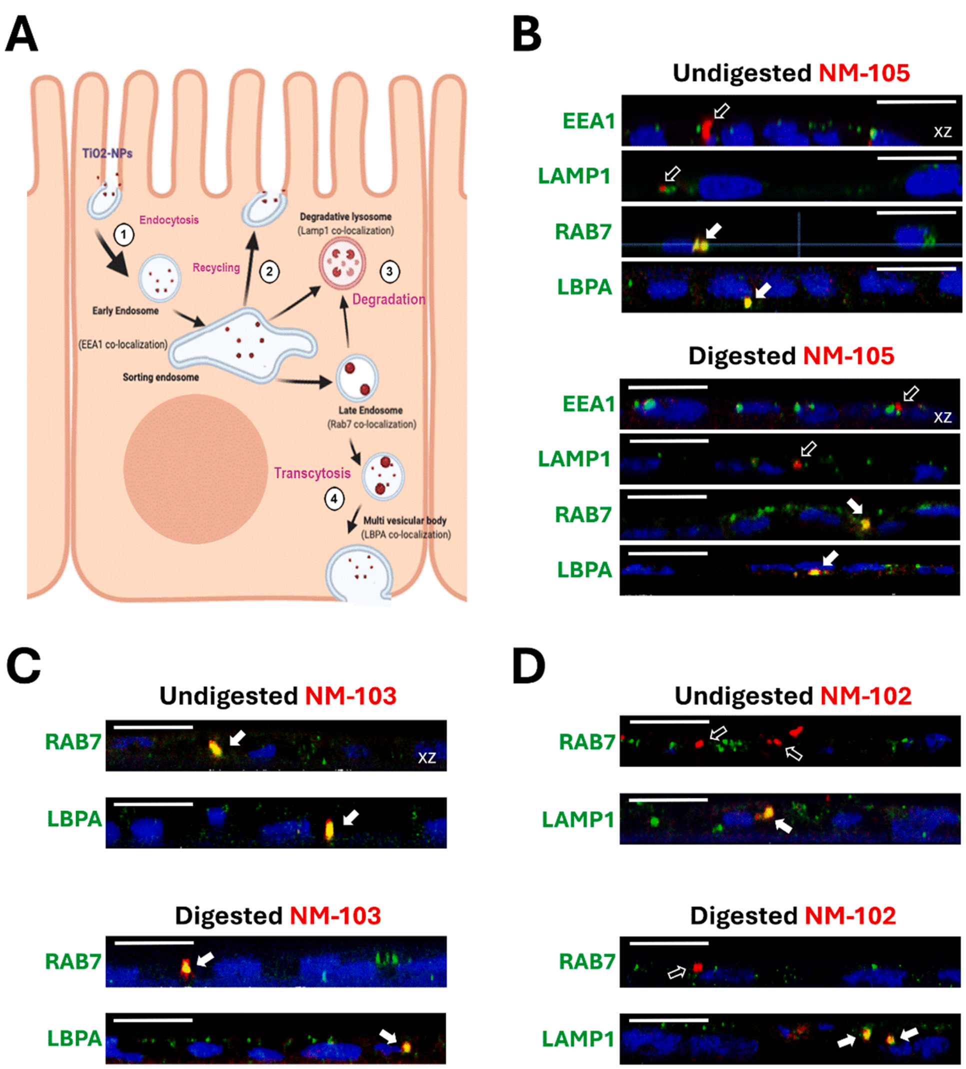

Fig. 3. Subcellular localization of TiO_2-NMs internalized by polarized Caco-2 cells. (A) Diagram illustrating potential endocytic pathways of internalized TiO_2-NMs in Caco-2 cells: 1) entry via endocytosis into early endosomes (co-localization with EEA1); 2) recycling back to the apical membrane from the sorting endosomal compartment; 3) sorting for degradation in lysosomes (co-localization with LAMP1); 4) routing to late endosomes and multivesicular bodies (co-localization with RAB7 and LBPA), followed by exocytosis at the basolateral membrane (apical-to-basolateral transcytosis). Model created with BioRender.com. (B-D) Confocal images showing XZ cross-sections of polarized Caco-2 monolayers after 24-h exposure to 14 μg/mL of either digested or undigested TiO_2-NMs conjugated to Alizarin-red (red signals). Cells were labeled with antibodies against EEA1, LAMP1, RAB7, or LBPA (green signals), and nuclei were stained with DAPI (blue signals). Filled arrows indicate co-localization of TiO_2-NMs with the respective compartment marker (yellow signals). Hollow arrows denote the absence of co-localization. White horizontal bars represent 25 μm.

TiO_2-NMs compromise epithelial integrity on human intestinal epithelial cells (Xu et al. 2021). To further confirm these observations, we examined the expression of epithelial markers after NM exposure. Western blot analysis of lysates from these monolayers showed no significant changes in the levels of the epithelial markers E-cadherin and ZO-1 (Fig. 2D), well-established epithelial markers for the integrity of adherens and tight junctions, respectively, previously reported to be downregulated after exposure to TiO_2-NMs (Koeneman, et al. 2010; Farcal et al. 2015; Jones et al. 2015). These discrepancies might be dose-dependent or related to differences in physicochemical properties between different TiO_2-NMs.

Here, we show that all tested TiO_2-NMs are internalized by mucous-producing HT29-MTX-E12 cells and polarized Caco-2 enterocytes, but not in undifferentiated Caco-2. Furthermore, 24 h exposure at physiological concentrations of TiO_2-NMs (14 μg/mL) either digested or not, do not appear to compromise the epithelial barrier integrity in polarized Caco-2 enterocytes.

3.3. Transcytosis of TiO_2-NMs in polarized enterocytes

When TiO_2-NMs reach the enterocyte apical membrane, they can interact with components of the plasma membrane or other extracellular medium components and enter the cell, mainly through endocytosis (Behzadi et al. 2017; Pridgen et al. 2014; Zhu et al. 2016). The path of the NMs along these pathways can be followed through their co-localization with markers associated with the different endosomal compartments (Fig. 3A), namely, EEA1 for early/sorting endosomes, LAMP1 for lysosomes, RAB7 for late endosomes and LBPA for multiple vesicular bodies (MVBs) (Murphy et al. 2005; Xia et al. 2016). Using confocal fluorescence microscopy, we tracked the subcellular localization of the agglomerates formed by each of the three TiO_2-NMs inside the polarized Caco-2 monolayers.

We started with NM-105, comparing the digested and undigested forms, as we previously found that its physical properties were most significantly altered by the INFOGEST 2.0 digestion procedure (Bettencourt et al., 2020). Curiously, we observed that in polarized Caco-2 cells, both forms of this NM accumulated in intercellular agglomerates co-localizing with RAB7 and LBPA but not with EEA1 or with LAMP1 (Fig. 3B), suggesting that upon uptake NM-105 could be following the transcytosis pathway. Intracellular digested and undigested NM-103 agglomerates also co-localized with RAB7 and LBPA (Fig. 3C). Interestingly, both digested and undigested NM-102 did not co-localize with RAB7 or LBPA but rather with LAMP1 (Fig. 3D), suggesting that, in contrast to the other two NMs, internalized NM-102 appears to accumulate within the degradative lysosomal compartment. Taken together, results suggest that NM-105 and NM-103 could be translocated through the epithelial monolayer by transcytosis, while NM-102 appears to be trapped intracellularly within the lysosomal compartment after endocytosis.

To investigate this, we tracked the epithelial translocation of Alizarin-labeled TiO_2-NMs by measuring changes in fluorescence in the medium from the apical (AP) to the basolateral (BL) compartments of polarized cells. For practical reasons and in line with other studies (Déciga-Alcaraz, 2020), we assumed that the dye does not significantly alter the intrinsic properties of the TiO2-NMs. However, after 24 h of exposure to 14 μg/mL of each labeled TiO_2-NMs, whether digested or not, we did not detect enough fluorescence to effectively evaluate significant changes in NM abundance between the apical (AP) and basolateral (BL) compartments (Fig. 4A). We hypothesized that this could be due to the reduced NM concentrations used and thus repeated the experiments with the NMs at 100 μg/mL. Under these conditions, we readily observed a significant decrease in AP fluorescence and a corresponding increase BL fluorescence 24 h after exposure to digested NM-105 and NM-103 (Fig. 4B). From these observations, the simplest explanation is that no passage of TiO2-NMs occurs at low doses, only at higher, supra-physiological concentrations.

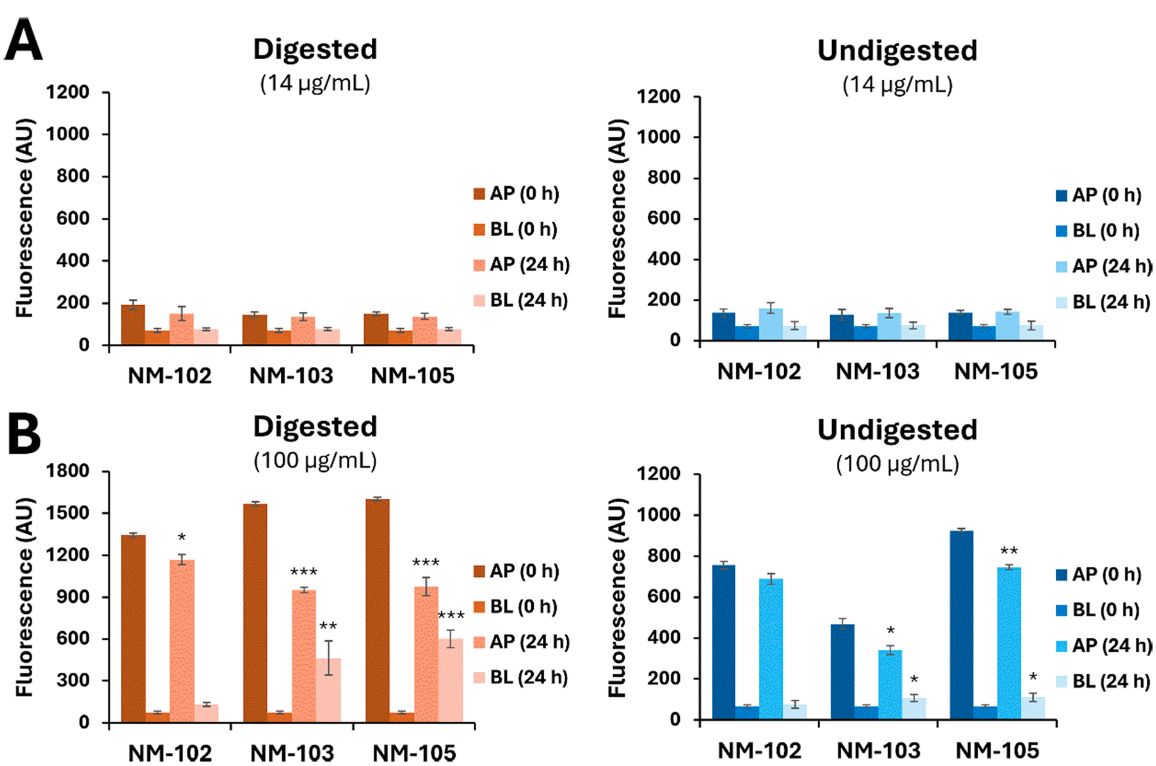

Fig. 4. Analysis of TiO_2-NM translocation through polarized Caco-2 monolayers. Fluorescence in the medium was measured in the apical (AP) and basolateral (BL) compartments at the time of exposure (0 h) and after 24 h of exposure to either (A) 14 μg/mL or (B) 100 μg/mL of digested or undigested TiO_2-NMs (as indicated). The plots show mean fluorescence values (± SD) from at least three independent experiments. Statistical significance is denoted as follows: (*) $p < 0.05$, (**) $p < 0.01$, and (***) $p < 0.001$, comparing fluorescence levels at 0 h and 24 h in the same compartment.

A similar, though less pronounced, trend was also seen with the undigested forms of these NMs (Fig. 4B). Regarding NM-102, although we observed a slight decrease in AP fluorescence 24 h after exposure, particularly with the digested form, no significant fluorescence signals were detected in the BL compartment for either the digested or undigested forms (Fig. 4B).

These findings are consistent with the microscopy observations, indicating that internalized NM-102 is retained in the lysosomal compartment, whereas NM-105 and NM-103 are transcytosed across the epithelial barrier of polarized Caco-2 enterocytes, reaching the basolateral side. The observation that NM-102 is trapped in the lysosomes, thus potentially damaging the cells could suggest an autophagy interference, comparable with other NMs that are trapped in the lysosomal compartment (e.g. SiO2). In fact, in a recent publication (Abulikemu et al., 2022) states that internalized Silica NMs accumulated in the lysosomes, caused lysosomal dysfunction, increased lysosomal membrane permeability and resulting in autophagy dysfunction.

Our findings reinforce previous reports confirming that subtle differences in the properties of TiO_2-NMs can lead to different cellular outcomes (Vieira et al., 2022). However, it is important to highlight the challenge of identifying which small differences in specific physicochemical properties account for the varying cellular fates between digested and undigested NMs. For instance, in a previous study, we extensively investigated the effects of *in vitro* simulated digestion on the physicochemical properties of non-fluorescent TiO_2-NMs. This study employed a comprehensive set of analytical techniques to assess post-digestion changes, including dynamic light scattering (DLS), electrophoretic light scattering (Zeta potential), and transmission electron microscopy (TEM). Our findings indicated that the digestion process did not result in significant alterations to the overall physicochemical properties of the NMs. However, while the overall particle size and surface charge remained stable after digestion, subtle changes in the agglomeration state of NM-105 were observed, which were associated with increased cytotoxicity in intestinal cells. Moreover, our observations suggest that despite not causing immediate damage, the physicochemical properties of the TiO_2-NMs were possibly modified by the digestion process, eliciting subtle effects on the way they interact with epithelial cells, namely in their ability to move across the epithelial barrier.

This may be particularly important in the context of cumulative exposure. Deposition of TiO_2-NMs in mouse organs has been previously shown in liver and spleen, suggesting potential bioaccumulation of concern if chronic/continuous exposure occurs (Louro et al. 2014). Other authors have also stated that TiO_2-NMs accumulation in Caco-2 cells is crystal structure-dependent, and that the mechanism involves endocytosis (Gitrowski et al. 2014).

Extended accumulation of TiO_2-NMs was shown to compromised lysosomal membrane stability in skin, lung, and gastric epithelial cells, resulting in significant cytotoxicity (Azimee et al. 2020; Kim et al. 2021; Kononenko and Drobne, 2019). One could therefore infer that long term exposure to NM-102 could also result in lysosomal damage and increased cytotoxicity in intestinal cells.

Very low translocation was reported in a differentiated Caco-2 monolayer system exposed to newly synthesized spherical TiO_2-NMs (18 ± 8 nm; surface area 89.8 m^2/g) (Janer et al., 2014). However, differences in the physicochemical properties of the NMs used may justify the different effects observed on the intestinal barrier integrity. In our previous work, only one of the tested TiO_2, the anatase-rutile (NM-105), induced cell death or mild DNA damage, suggesting that crystallinity is critical determinant of TiO_2 toxicity. We have also demonstrated that digested NM-105 showed a better dispersion, and the mean size was significantly lower than the undigested NM-105 sample (Bettencourt et al., 2020).

3.4. Potential pro-inflammatory effects of TiO2-NMs

Since we found NM-103 and NM-105 able to cross the epithelial barrier through transcytosis, we next asked whether the presence of these NMs at the basolateral interstice could challenge immune cells, such as macrophages (Fig. 5A), that *in vivo* patrol the *lamina propria* beneath the intestinal epithelium (Ruder and Becker, 2020).

We observed that, unlike the response to LPS and IFN-γ (Fig. 5B), neither the digested nor undigested forms of the two NMs, regardless of concentration, significantly affected *IL1B* transcript abundance in differentiated M0 cells (Fig. 5C). This suggests that the NMs alone were insufficient to activate macrophages. However, we observed that 14 μg/mL of digested, but not of undigested, NM-105 significantly upregulated IL-1β expression in activated M1 macrophages (Fig. 5D). Moreover, the effect was still observable, and only slightly less pronounced, when the cells were exposed to a ten times lower NM concentration (1.4 μg/mL; Fig. 5D), indicating that exposure to even very low concentrations of digested NM-105 might induce the pro-inflammatory response of activated macrophages. In contrast, neither form of NM-103 produced a significant change in IL1β transcript levels in M1 cells.

The observation that the digestion process made NM-105 more prone to challenge M1 macrophages, may be related to differences in the NM physicochemical properties. In fact, previous studies reported that the digestion process influenced the mean average size of this TiO_2-NM in the biological medium, and were also associated to increased cytotoxicity (Bettencourt et al., 2020). In addition, this observation also suggests that upon transcytosis, NM-105 would be in position to locally stimulate immune cells patrolling the GIT and, if systemically distributed, influence the inflammatory response in other organs and tissues. Consistently, exposure of patrolling immune cells to TiO_2-NMs has been reported to promote the expression of pro-inflammatory cytokines, including IL-1β (Evans et al. 2002; Huang et al. 2017), being frequently accompanied by increased inflammassome activation (Azim et al. 2015; Ruiz et al. 2017; Tada-Oikawa et al. 2016; Winter et al. 2011; Watari et al. 2008; Powell et al. 2000; Heller et al. 2018). Moreover, there are several *in vivo* studies reporting systemic inflammatory effects related to TiO_2-NMs exposure, leading to liver injury, reproductive toxicity, cardiac and kidney damage, as well as deleterious hematological effects (Rolo et al. 2022).

It should be noted that our results were not consistent across all three TiO_2-NMs, which indicates that the specific physicochemical properties of each NM and their interaction with their surrounding media have a significant impact on their biological effects and a case-by-case assessment has to be considered. Moreover, while suggestive of a pro-inflammatory response, our preliminary analysis of IL-1β expression requires further strengthening. Therefore, future investigation into inflammasome activation and IL-1β secretion in this model is essential to more comprehensively evaluate the biological response to TiO_2 exposure.

4. Conclusions

Our study provides new insights into the potential mechanisms associated with the ingestion of TiO_2-NMs that may underlie reported adverse outcomes (Vieira et al. 2022). Our findings indicate that some TiO_2-NMs can cross the colonic epithelial barrier via transcytosis without causing damage to the intestinal barrier, while others are internalized and accumulate inside intestinal cells, being the effect dependent on the characteristics of the TiO_2-NMs. Upon transcytosis, some TiO_2-NMs influence the inflammatory response both in GIT and in other organs and tissues, after systemic distribution. These observations complement the key events identified in previously proposed AOPs, which suggests that oral exposure to TiO_2-NMs can lead to a range of both GIT and systemic harmful effects (Rolo et al. 2022). A new AOP (AOP 530) was recently proposed for food nanomaterial-induced intestinal barrier disruption (Stanco et al., 2024). AOP 530 starts with

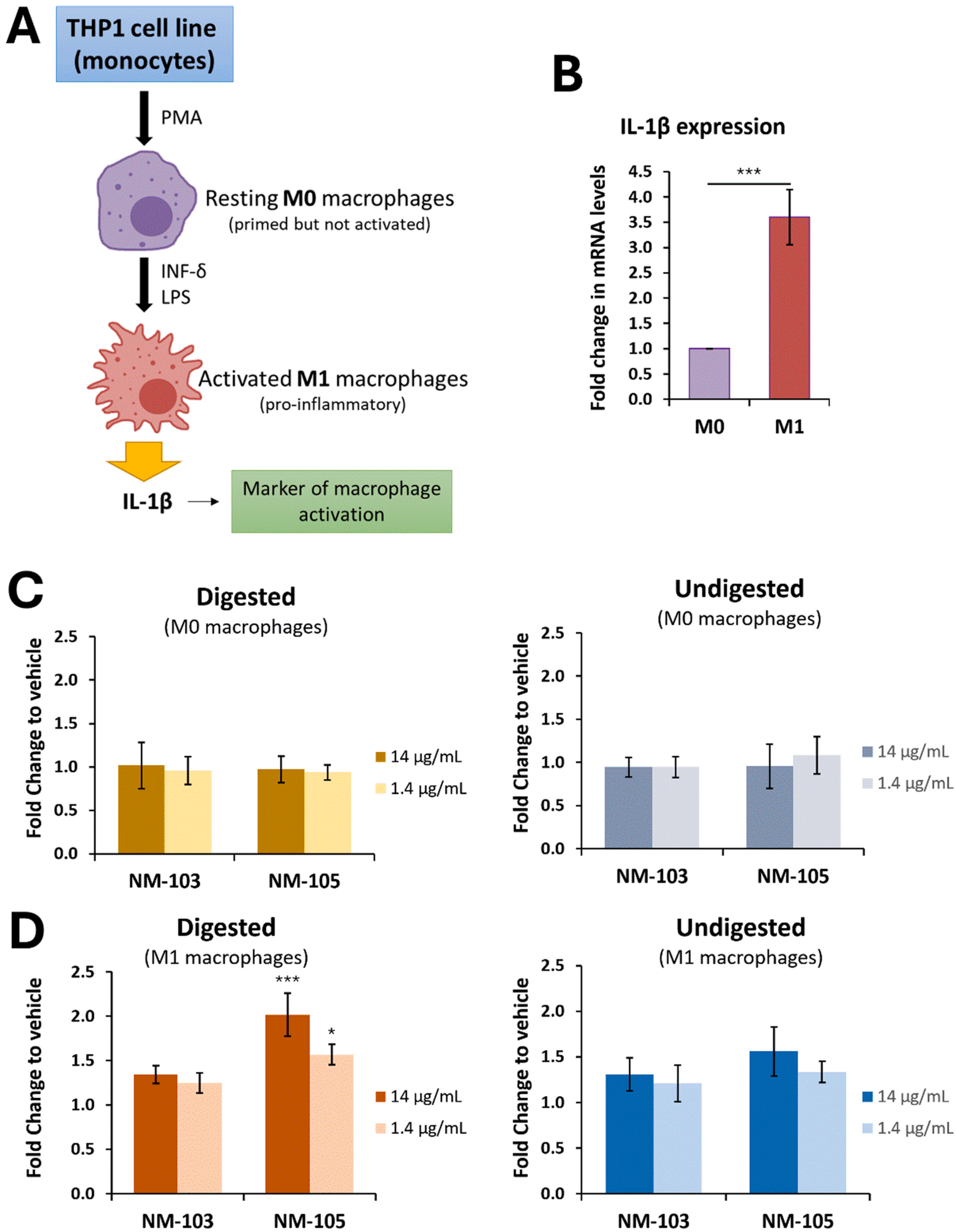

Fig. 5. Effect of TiO_2-NM exposure on IL-1β expression in human macrophages. (A) Diagram illustrating the *in vitro* differentiation of THP1 human monocytes into resting M0 macrophages and pro-inflammatory M1 macrophages (Created with BioRender.com). (B) Comparison of *IL1B* transcript levels between M0 and M1 differentiated macrophages. Data are presented as means ± SD from 8 independent assays. (C) Differentiated M0 and (D) M1 macrophages were either mock exposed or exposed for 24 h to two concentrations (14 and 1.4 μg/mL) of the indicated digested or undigested TiO_2-NMs. *IL1B* transcript levels were measured as in (B) and are expressed as fold change relative to the mock-exposed condition of the respective macrophage subtype. Data represent means ± SD from five independent assays. Statistical significance is indicated as follows: (*) $p < 0.05$ and (***) $p < 0.001$.

endocytic lysosomal uptake, its disruption may lead to mitochondrial dysfunction, causing cell death/injury, which will drive the intestinal barrier disruption via increased paracellular permeability and/or via decreased mucus production. The work supports that food-related NMs can be taken up by intestinal cells and indicates that intestinal barrier disruption may occur due to several NMs, but no conclusion was obtained for TiO2-NMs (Stanco et al., 2024).

In addition, this study contributes to the weight of evidence supporting the need to limit their use in food, in line with the decision by the European Food Safety Authority (EFSA, 2021). In addition, our findings also raise concerns about the potential adverse effects of TiO_2-NMs used in pharmaceuticals or in personal hygiene products that lead to oral exposure. In view of the different outcomes for closely related TiO_2 NPs, the specific physicochemical properties of each NM and their interaction with their surrounding media have a significant impact on their biological effects and a case-by-case assessment should to be considered, while full understanding of the factors that determine NMs uptake and biokinetics is not clarified.

Therefore, further research is needed to fully understand the risks associated with the use of TiO_2-NMs in various products that imply ingestion, to support the development of regulation to minimize their potential harm to human health.

CRediT authorship contribution statement

Rolo Dora: Writing – original draft, Methodology, Investigation, Data curation. **Gonçalves Lídia:** Writing – review & editing, Visualization, Investigation. **Joana F. S. Pereira:** Writing – review & editing, Validation, Methodology, Investigation, Conceptualization. **Jordan Peter:** Writing – review & editing, Supervision, Investigation, Formal analysis, Conceptualization. **Bettencourt Ana:** Writing – review & editing, Supervision, Investigation. **Silva Maria João:** Writing – review & editing, Supervision, Investigation, Funding acquisition. **Louro Henriqueta:** Writing – review & editing, Supervision, Investigation, Funding acquisition, Conceptualization. **Matos Paulo:** Writing – review & editing, Writing – original draft, Validation, Supervision, Methodology, Investigation, Conceptualization.

Declaration of Competing Interest

The authors declare that they have no known competing financial interests or personal relationships that could have appeared to influence the work reported in this paper.

Acknowledgments

The authors thank all the support from the colleagues Paula Alvito, Carla Martins and Ricardo Assunção (Food Safety Department, INSA, Lisbon, Portugal) as well from all INGESTnano team members.

The Joint Research Centre (JRC, Ispra, Italy) is acknowledged for kindly providing the NMs for the study.

This work was funded by national funds through the FCT - Foundation for Science and Technology, I.P., under the project PTDC/SAU-PUB/29481/2017. Research was co-funded by ToxOmics (UIDB/00009/2020 and UIDP/00009/2020), BioISI (UID/MULTI/04046/2019), iMed.ULisboa (UIDB/04138/2020 and UIDP/04138/2020), and principal investigator contract CEECIND/03143/2017 (L.G.).

Appendix A. Supporting information

Supplementary data associated with this article can be found in the online version at doi:10.1016/j.tox.2025.154066.

Data availability

Data will be made available on request.

References

Abulikemu, A., et al., 2022. Lysosomal impairment-mediated autophagy dysfunction responsible for the vascular endothelial apoptosis caused by silica nanoparticle via ROS/PARP1/AIF signaling pathway. Environ. Pollut. 304 (2022), 119202. https://doi.org/10.1016/j.envpol.2022.119202.

Azim, S.A.A., Darwish, H.A., Rizk, M.Z., Ali, S.A., Kadry, M.O., 2015. Amelioration of titanium dioxide nanoparticles-induced liver injury in mice: possible role of some antioxidants. Exp. Toxicol. Pathol. 67 (4), 305–314. https://doi.org/10.1016/j.etp.2015.02.001.

Azimee, S., Rahmati, M., Fahimi, H., Moosavi, M.A., 2020. TiO(2) nanoparticles enhance the chemotherapeutic effects of 5-fluorouracil in human AGS gastric cancer cells via autophagy blockade. Life Sci. 248, 117466. https://doi.org/10.1016/j.lfs.2020.117466.

Behzadi, S., et al., 2017. Cellular uptake of nanoparticles: journey inside the cell. Chem. Soc. Rev. 46 (14), 4218–4244. https://doi.org/10.1039/c6cs00636a.

Bettencourt, A., et al., 2020. Analysis of the characteristics and cytotoxicity of titanium dioxide nanomaterials following simulated in vitro digestion. Nanomaterials 10 (8), 1516. https://doi.org/10.3390/nano10081516.

Brodkorb, A., et al., 2019. INFOGEST static in vitro simulation of gastrointestinal food digestion. Nat. Protoc. 14 (4), 991–1014. https://doi.org/10.1038/s41596-018-0119-1.

Cao, X., et al., 2019. Impact of protein-nanoparticle interactions on gastrointestinal fate of ingested nanoparticles: not just simple protein corona effects. NanoImpact 13, 37–43. https://doi.org/10.1016/j.impact.2018.12.002.

Costa, J., Ahluwalia, A., 2019. Advances and current challenges in intestinal in vitro model engineering: a digest. Front Bioeng. Biotechnol. 7, 144. https://doi.org/10.3389/fbioe.2019.00144.

Déciga-Alcaraz, A., et al., 2020. Toxicity of engineered nanomaterials with different physicochemical properties and the role of protein corona on cellular uptake and intrinsic ROS production. Toxicology 442, 152545. https://doi.org/10.1016/j.tox.2020.152545.

EFSA, 2021. Safety assessment of titanium dioxide (E171) as a food additive, 19. EFSA J. (5), e06585. https://doi.org/10.2903/j.efsa.2021.6585.

Evans, S.M., Ashwood, P., Warley, A., Berisha, F., Thompson, R.P., Powell, J.J., 2002. The role of dietary microparticles and calcium in apoptosis and interleukin-1beta release of intestinal macrophages. Gastroenterology 123 (5), 1543–1553. https://doi.org/10.1053/gast.2002.36554.

Farcal, L., et al., 2015. Comprehensive in vitro toxicity testing of a panel of representative oxide nanomaterials: first steps towards an intelligent testing strategy. PLoS One 10 (5), e0127174. https://doi.org/10.1371/journal.pone.0127174.

Gitrowski, C., Al-Jubory, A.R., Handy, R.D., 2014. Uptake of different crystal structures of TiO_2 nanoparticles by Caco-2 intestinal cells. Toxicol. Lett. 226 (3), 264–276. https://doi.org/10.1016/j.toxlet.2014.02.014.

Heller, A., Jarvis, K., Coffman, S., 2018. Association of type 2 diabetes with submicron titanium dioxide crystals in the pancreas. Chem. Res Toxicol. 31 (6), 506–509. https://doi.org/10.1021/acs.chemrestox.8b00047.

Huang, C., et al., 2017. Titanium dioxide nanoparticles prime a specific activation state of macrophages. Nanotoxicology 11 (6), 737–750. https://doi.org/10.1080/17435390.2017.1349202.

Huang, Y., Mei, L., Chen, X., Wang, Q., 2018. Recent developments in food packaging based on nanomaterials. Nanomaterials 8 (10). https://doi.org/10.3390/nano8100830.

Iftikhar, M., Iftikhar, A., Zhang, H., Gong, L., Wang, J., 2020. Transport, metabolism and remedial potential of functional food extracts (FFEs) in Caco-2 cells monolayer: a review. Food Res. Int. 136, 109240. https://doi.org/10.1016/j.foodres.2020.109240.

Jones, K., Morton, J., Smith, I., Jurkschat, K., Harding, A.H., Evans, G., 2015. Human in vivo and in vitro studies on gastrointestinal absorption of titanium dioxide nanoparticles. Toxicol. Lett. 233 (2), 95–101. https://doi.org/10.1016/j.toxlet.2014.12.005.

Kim, I.Y., Lee, T.G., Reipa, V., Heo, M.B., 2021. Titanium dioxide induces apoptosis under UVA irradiation via the generation of lysosomal membrane permeabilization-dependent reactive oxygen species in HaCat cells. Nanomaterials 11 (8). https://doi.org/10.3390/nano11081943.

Koch, S., Nusrat, A., 2009. Dynamic regulation of epithelial cell fate and barrier function by intercellular junctions. Ann. N. Y Acad. Sci. 1165, 220–227. https://doi.org/10.1111/j.1749-6632.2009.04025.x.

Koeneman, B.A., Zhang, Y., Westerhoff, P., Chen, Y., Crittenden, J.C., Capco, D.G., 2010. Toxicity and cellular responses of intestinal cells exposed to titanium dioxide. Cell Biol. Toxicol. 26 (3), 225–238. https://doi.org/10.1007/s10565-009-9132-z.

Kononenko, V., Drobne, D., 2019. In vitro cytotoxicity evaluation of the magnéli phase titanium suboxides (Ti(x)O(2x-1)) on A549 human lung cells. Int. J. Mol. Sci. 20 (1). https://doi.org/10.3390/ijms20010196.

Louro, H., et al., 2014. Integrated approach to the in vivo genotoxic effects of a titanium dioxide nanomaterial using LacZ plasmid-based transgenic mice. Environ. Mol. Mutagen 55 (6), 500–509. https://doi.org/10.1002/em.21864.

Malaisé, Y., et al., 2024. Validating enteroid-derived monolayers from murine gut organoids for toxicological testing of inorganic particles: proof-of-concept with food-grade titanium dioxide. Int. J. Mol. Sci. 25 (5). https://doi.org/10.3390/ijms25052635.

Murphy, A.S., Bandyopadhyay, A., Holstein, S.E., Peer, W.A., 2005. Endocytotic cycling of PM proteins. Annu Rev. Plant Biol. 56, 221–251. https://doi.org/10.1146/annurev.arplant.56.032604.144150.

Pereira, J.F.S., Bessa, C., Matos, P., Jordan, P., 2022. Pro-inflammatory cytokines trigger the overexpression of tumour-related splice variant RAC1B in polarized colorectal cells. Cancers 14 (6). https://doi.org/10.3390/cancers14061393.

Powell, J.J., Harvey, R.S., Ashwood, P., Wolstencroft, R., Gershwin, M.E., Thompson, R. P., 2000. Immune potentiation of ultrafine dietary particles in normal subjects and patients with inflammatory bowel disease. J. Autoimmun. 14 (1), 99–105. https://doi.org/10.1006/jaut.1999.0342.

Pridgen, E.M., Alexis, F., Farokhzad, O.C., 2014. Polymeric nanoparticle technologies for oral drug delivery. Clin. Gastroenterol. Hepatol. 12 (10), 1605–1610. https://doi.org/10.1016/j.cgh.2014.06.018.

Rice, P.A., 2022. Toxicity of Nanomaterials to the Gastrointestinal Tract (Toxicology of Nanoparticles and Nanomaterials in Human, Terrestrial and Aquatic Systems). John Wiley & Sons, Inc. https://doi.org/10.1002/9781119316329.ch12.
Rolo, D., et al., 2022. Adverse outcome pathways associated with the ingestion of titanium dioxide nanoparticles-a systematic review. Nanomaterials 12 (19). https://doi.org/10.3390/nano12193275.
Ruder, B., Becker, 2020. At the forefront of the mucosal barrier: the role of macrophages in the intestine. Cells 9 (10). https://doi.org/10.3390/cells9102162.
Ruiz, P.A., et al., 2017. Titanium dioxide nanoparticles exacerbate DSS-induced colitis: role of the NLRP3 inflammasome. Gut 66 (7), 1216–1224. https://doi.org/10.1136/gutjnl-2015-310297.
Shukla, R.K., Kumar, A., Vallabani, N.V.S., Pandey, A.K., Dhawan, A., 2014. Titanium dioxide nanoparticle-induced oxidative stress triggers DNA damage and hepatic injury in mice. Nanomedicine 9 (9), 1423–1434. https://doi.org/10.2217/nnm.13.100.
Stanco, D., Lipsa, D., Bogni, A., Bremer-Hoffmann, S., Clerbaux, L.A., 2024 Dec 24. An adverse outcome pathway for food nanomaterial-induced intestinal barrier disruption. Front. Toxicol. 6, 1474397. https://doi.org/10.3389/ftox.2024.1474397.
Tada-Oikawa, S., et al., 2016. Titanium dioxide particle type and concentration influence the inflammatory response in Caco-2 cells. Int. J. Mol. Sci. 17 (4), 576. https://doi.org/10.3390/ijms17040576.
Talbot, P., Radziwill-Bienkowska, J.M., Kamphuis, J.B.J., Steenkeste, K., Bettini, S., Robert, V., Noordine, M.L., Mayeur, C., Gaultier, E., Langella, P., Robbe-Masselot, C., Houdeau, E., Thomas, M., Mercier-Bonin, M., 2018. Food-grade TiO2 is trapped by intestinal mucus in vitro but does not impair mucin O-glycosylation and short-chain fatty acid synthesis in vivo: implications for gut barrier protection. Jun 19 J. Nanobiotechnology 16 (1), 53. https://doi.org/10.1186/s12951-018-0379-5.
Thurn, K.T., et al., 2009. Labeling TiO2 nanoparticles with dyes for optical fluorescence microscopy and determination of TiO2-DNA nanoconjugate stability. Small 5 (11), 1318–1325. https://doi.org/10.1002/smll.200801458.
Vieira, A., et al., 2022. Investigation of the genotoxicity of digested titanium dioxide nanomaterials in human intestinal cells. Food Chem. Toxicol. 161, 112841. https://doi.org/10.1016/j.fct.2022.112841.
Vignard, J., et al., 2023. Food-grade titanium dioxide translocates across the buccal mucosa in pigs and induces genotoxicity in an in vitro model of human oral epithelium. Nanotoxicology 17 (4), 289–309. https://doi.org/10.1080/17435390.2023.2210664.
Vital, N., et al., 2024. Challenges of the application of in vitro digestion for nanomaterials safety assessment. Foods 13 (11). https://doi.org/10.3390/foods13111690.
Watari, F., et al., 2008. Behavior of in vitro, in vivo and internal motion of micro/nano particles of titanium, titanium oxides and others. J. Ceram. Soc. 116 (1349), 1–5. https://doi.org/10.2109/jcersj2.116.1.
Winter, M., Beer, H.D., Hornung, V., Krämer, U., Schins, R.P., Förster, I., 2011. Activation of the inflammasome by amorphous silica and TiO2 nanoparticles in murine dendritic cells. Nanotoxicology 5 (3), 326–340. https://doi.org/10.3109/17435390.2010.506957.
Xia, L., et al., 2016. Endocytosed nanoparticles hold endosomes and stimulate binucleated cells formation. Part Fibre Toxicol. 13 (1), 63. https://doi.org/10.1186/s12989-016-0173-1.
Xu, K., Basu, N., George, S., 2021. Dietary nanoparticles compromise epithelial integrity and enhance translocation and antigenicity of milk proteins: an in vitro investigation. NanoImpact 24, 100369. https://doi.org/10.1016/j.impact.2021.100369.
Zhu, X., et al., 2016. Polymeric nanoparticles amenable to simultaneous installation of exterior targeting and interior therapeutic proteins. Angew. Chem. Int. Ed. 55 (10), 3309–3312. https://doi.org/10.1002/anie.201509183.